Optical Society of America. Vinh Q. Nguyen, Jas S. Sanghera, Frederic H. Kung, Ishwar D. Aggarwal, and Isabel K. Lloyd, "Effect of Temperature on the Absorption Loss of Chalcogenide Glass Fibers," Appl. Opt. 38, 3206-3213 (1999). doi: 10.1364/ao.38.003206

Effect of temperature on the absorption loss of chalcogenide glass fibers

Vinh Q. Nguyen, Jas S. Sanghera, Frederic H. Kung, Ishwar D. Aggarwal, and Isabel K. Lloyd

The change in the absorption loss of IR-transmitting chalcogenide glass fibers in the temperature range of $-90\ ^\circ\mathrm{C} \le T \le 70\ ^\circ\mathrm{C}$ was investigated. For sulfur-based glass fibers the change in loss relative to room temperature was slightly affected by the temperature in the wavelength region of 1–5 μm. For $\lambda \ge 6$ μm the change in loss was mainly due to multiphonon absorption. The change in loss for tellurium-based glass fibers increased significantly at $T = 60\ ^\circ\mathrm{C}$. The increase in the loss at short wavelengths ($\lambda \le 4.1$ μm) was due to electronic excitations in the tail states. Between 5 and 9 μm there was noticeable free-carrier absorption. Beyond $\lambda \ge 9$ μm, multiphonon absorption dominated the loss spectrum.

OCIS codes: 060.2280, 060.2310, 060.2390, 060.2290, 060.2270.

1. Introduction

Silica and fluoride optical glasses have limited use because these glasses do not transmit much beyond 2 and 3 μm, respectively, owing to multiphonon absorption.[1] Chalcogenide glasses have received a great deal of attention owing to their wide range of IR transmission, typically from 1 to 13 μm.[1] Chalcogenide glasses are made from mixtures of chalcogen elements, S, Se, and Te. The addition of network formers such as germanium, arsenic, and antimony establishes cross-linking between the tetrahedral and the pyramidal units, which facilitates stable glass formation. The chalcogenide glasses are stable against crystallization, are chemically inert, have excellent thermal stability, and are relatively easy to fiberize. Chalcogenide optical fibers are currently being used in laser power delivery (e.g., CO at 5.4 μm and CO_2 at 10.6 μm) as well as in fiber-optic chemical sensor systems using absorption, evanescent, and diffusive reflectance spectroscopy for environmental and Department of Defense facility cleanup.[2–5] In addition these fibers are used in IR countermeasure and laser threat-warning systems to enhance aircraft survivability.[6]

We have developed and fabricated stable low-loss IR-transmitting chalcogenide glass fibers that transmit to beyond 10 μm. Improved purification and processing techniques have been used to fabricate low-loss tellurium-containing fiber ($Ge_{30}As_{10}Se_{30}Te_{30}$) that transmits in the 2–10-μm region with a loss of 0.11 dB/m at 6.6 μm.[7] Similarly, arsenic-sulfide-based fibers that transmit in the 1–6.5-μm region have been obtained with losses of less than 0.1 dB/m at lengths of as many as 50 m.[8] Since low-loss chalcogenide fibers now enable numerous applications, the question arises as to whether their loss is affected by environmental changes, especially temperature. Therefore the objective of this paper is to investigate the temperature dependence of the absorption loss in the IR-transmitting region for telluride and sulfide fibers. Also for sulfide fibers the temperature dependence on the absorption of low-loss high-purity fiber was compared with that of high-loss low-purity fiber.

2. Experimental Methods

A. Fabrication of Telluride and Sulfide Optical Fibers

The compositions of the core and the clad for the telluride fiber were $Ge_{30}As_{10}Se_{30}Te_{30}$ and $Ge_{25}As_{12}Se_{40}Te_{23}$, respectively. For the sulfide fiber the core and the clad compositions were $As_{40}S_{55}Se_5$ and $As_{40}S_{60}$,

V. Q. Nguyen is with the Department of Electrical Engineering, Virginia Polytechnic Institute, Blacksburg, Virginia 24061. His mailing address is Optical Science Division, Code 5606.1, Naval Research Laboratory, Washington, D.C. 20375-5000; e-mail address is vnguyen@ccf.nrl.navy.mil. F. H. Kung is with the University of Maryland Research Foundation, Greenbelt, Maryland 20770. J. S. Sanghera and I. D. Aggarwal are with the Optical Science Division, Code 5606. Naval Research Laboratory, Washington, D.C. 20375-5000. I. K. Lloyd is with the Department of Materials and Nuclear Engineering, University of Maryland at College Park, College Park, Maryland 20742.

Received 30 July 1998; revised manuscript received 26 January 1999.
0003-6935/99/153206-08$15.00/0

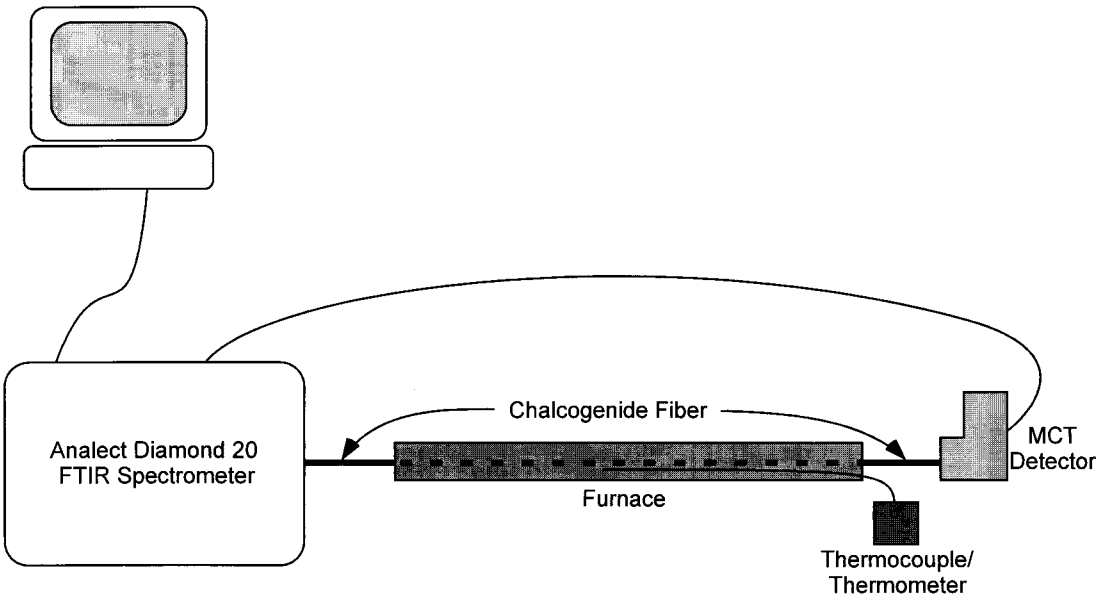

Fig. 1. Experimental setup for measuring heating effects on chalcogenide fiber.

respectively. The telluride and the sulfide fibers were made from high-purity rods and tubes. Commercially available 99.9999% purity of arsenic, selenium, and tellurium were baked at 450 °C, 300 °C, and 475 °C, respectively, for 8 h to remove appropriate oxide impurities such as As_2O_3, As_2O_5, SeO_2, SeO_3, Se_2O_3, TeO, and TeO_3. The arsenic and selenium were distilled further to remove scattering centers such as carbon, quartz particles, residual trapped gases, and other extraneous particles. The three times zone-refined Ge was used as received. The 99.9999% purity sulfur was distilled six times before use to remove trapped gases and particulate impurities.

High-quality quartz distillation ampoules were etched with 50/50 mol.% of hydrofluoric acid/deionized water for 2 min and then rinsed with deionized water several times. The ampoules were dried in a vacuum oven at 110 °C for 3 h. The chemicals were batched in these ampoules inside a glove box in a dry nitrogen atmosphere. To fabricate the core rods, we batched the ampoules containing the core composition by using purified chemicals. These ampoules were evacuated at 10^{-5} Torr for 5 h, sealed with an oxygen-methane torch, and placed in a two-zone furnace for melting. The melts were distilled and then remelted for homogenization. Approximately 10 ppm of elemental Al was added to the telluride batches to getter the oxygen impurities before distillation. All the glass melts were quenched and annealed from the glass-transition temperatures (205 and 265 °C for sulfide and telluride glass rods, respectively). Rods with cores of approximately 6-mm diameter and lengths as great as 12 cm were obtained. The processes of fabricating telluride and sulfide cladding tubes were similar except that the melts were spun at ~2500 rpm during cooling.[8] The cladding tubes were also annealed. The typical dimensions of the cladding tubes were approximately 6-mm inner diameter and 10-mm outer diameter. The fiberization was based on the rod-in-tube process. The sulfide and the telluride fibers were drawn between 330 and 400 °C at a rate of 0.5–2 m/min, depending on the required thickness of the fibers.[8] The sulfide and the telluride fibers were coated with poly(vinylidene fluoride) (PVF_2) and Teflon, respectively, to protect the fiber from abrasion. The diameters of the fiber core, cladding, and PVF_2 or Teflon jacket were 200, 330, and 370 μm, respectively. Low-quality arsenic-sulfide fibers were made with two times distilled sulfur.

B. Experimental Setup for Heating and Cooling the Fibers

Figure 1 shows the experimental setup used in measuring the relative change in transmission during heating with respect to room temperature. A fiber 1 m long was placed inside a cylindrical furnace 72 cm long with a 16-mm inner diameter. The ends of the furnace were closed off with insulation to minimize heat loss. The temperature inside the furnace was controlled uniformly so that the change in temperature along the length of the furnace was ±0.5 °C. The two 14-cm end sections of the fiber outside the furnace were exposed to room temperature during the measurement. During heating for each measurement the temperature was held at 10 min to achieve equilibrium. Figure 2 shows the experimental setup used in measuring the relative change in transmission during cooling with respect to room temperature. Inside a Styrofoam box 3 m of fiber was placed on top of a stainless-steel plate 1/16 in. (0.158 cm) thick suspended above a liquid nitrogen bath. Two thermocouples were used to monitor the

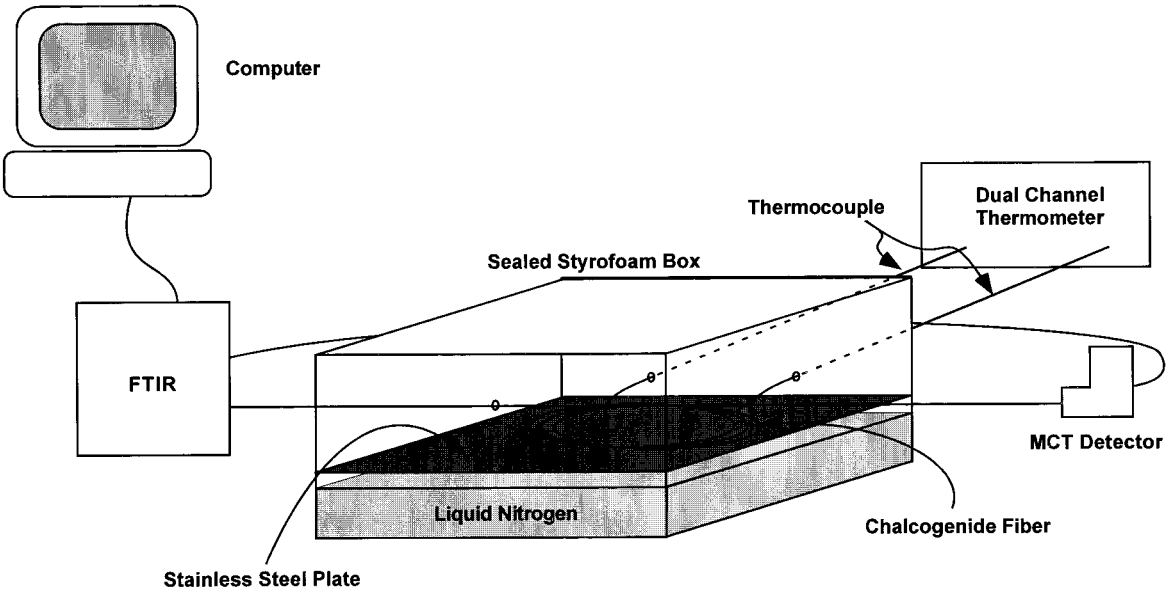

Fig. 2. Experimental setup for measuring cooling effects on chalcogenide fiber.

temperature. One was on the stainless-steel plate and the other was ~2 mm above the stainless-steel plate. The temperature readings from these two thermocouples were within ±1 °C. During cooling for each measurement the temperature was held for ~5 min to achieve equilibrium.

The relative change in transmission of a fiber caused by varying temperatures was determined by the following method. The ends of the fiber were connected to an Analect Diamond 20 Fourier-transform IR spectrometer. The intensity of the light transmitted through the fiber at room temperature $[I_0]$ was recorded and used as the reference for the measurement. The intensity $[I_T]$ of the transmitted light was recorded at specific temperatures as the fiber was either heated or cooled. The relative change in loss was calculated by

$$\text{relative } \Delta\text{loss (dB/m)} = -\frac{10}{l}\log[1 - |\Delta\text{trans}|] \times \frac{\Delta\text{trans}}{|\Delta\text{trans}|}, \quad (1)$$

where $\Delta\text{trans} = I_T/I_0$ and l is the length of the fiber in the heating/cooling zone.

C. Measurement of the Glass-Transition Temperature and the Optical Gap

Differential scanning calorimetry was used to determine the glass-transition temperature T_g for an ~40-mg glass sample of each composition at a heating rate of 10 °C/min under Ar gas. The absorption spectra near the electronic edge were measured with a Cary 5G spectrophotometer on 4-mm-thick samples with an optical finish on both endfaces. The absorption data were normalized with respect to the sample's thickness.

3. Results and Discussion

The fundamental optical gap of chalcogenide glasses can be determined from the spectral dependence of $\alpha(h\nu)$ with Tauc's relationship[9]:

$$(\alpha h\nu)^{1/2} = B(h\nu - E_0), \quad (2)$$

where α is the absorption coefficient (cm^{-1}), h is Planck's constant (eV s), ν is the frequency (s^{-1}), B is a material-dependent constant, and E_0 is the optical gap (eV). The intercept of $(\alpha h\nu)^{1/2}$ versus $h\nu$ yields the value of the optical gap. Figure 3 shows the plot of $(\alpha h\nu)^{1/2}$ as a function of photon energy $(h\nu)$ for the tellurium-containing glasses ($Ge_{30}As_{10}Se_{30}Te_{30}$ and $Ge_{25}As_{12}Se_{40}Te_{23}$) and sulfur-based glasses ($As_{40}S_{60}$ and $As_{40}S_{55}Se_5$) measured at room temperature. In Table 1 we list the optical gap and the glass-transition temperature for the sulfide and the telluride glasses. It is clearly evident that the telluride glasses possess lower optical gaps, and furthermore the selenium doping of the sulfide glasses reduces the optical gap of the sulfide glass.

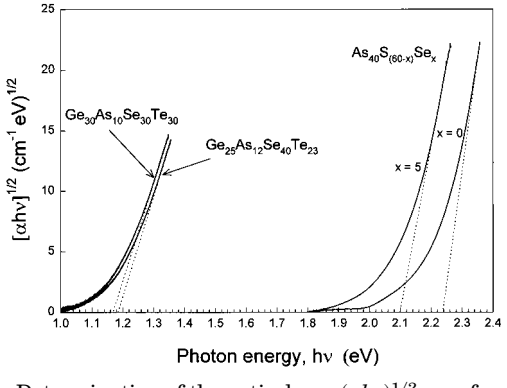

Fig. 3. Determination of the optical gap $(\alpha h\nu)^{1/2}$ as a function of photon energy $(h\nu)$.

Table 1. Optical and Thermal Properties of Telluride and Sulfide Glasses

Composition (at.%)	Optical Gap (22 °C) (eV)	Glass-Transition Temperature T_g (°C)
$As_{40}S_{60}$	2.25	201
$As_{40}S_{55}Se_5$	2.13	199
$Ge_{25}As_{12}Se_{40}Te_{23}$	1.18	268
$Ge_{30}As_{10}Se_{30}Te_{30}$	1.17	265

Figure 4 shows the change in loss of the sulfide fiber with increasing temperature. The absorption peak at 2.83 μm is due to the symmetric stretching vibration of H_2O molecules. The fiber becomes more transparent at 2.83 μm with increasing temperature, perhaps because of the diffusion of a physiadsorbed H_2O species at the fiber–PVF_2 interface out through the PVF_2 jacket. This increasing transparency is possible because of the weak secondary van der Waals bonding and the relatively open structure in PVF_2 whose structure consists of large chains of —CH_2CF_2— molecules. In fact as the temperature drops back to 20 °C the change in loss at 2.83 μm remains −0.12 dB/m, thereby confirming the diffusion of a physiadsorbed H_2O species through the PVF_2 jacket. At T = 70 °C there is a noticeable increase in the loss at ~3.5 μm, which is attributed to the presence of the PVF_2 coating. This increase is due to thermal energy that increases the vibration of the —CH_2CF_2— species, resulting in an increased loss. Overall the change in loss in the wavelength region from ~1.6 μm to 5 μm is affected only slightly by temperature. In addition a band centered at ~4.3 μm is attributed to CO_2 and decreases in intensity as the temperature rises, probably owing to desorption and then diffusion of physiadsorbed CO_2 gas at the fiber surface through the PVF_2 jacket. Similarly a small band at ~3.3 μm is attributed to C—H groups owing to the removal of organic impurities from the glass fiber surface.

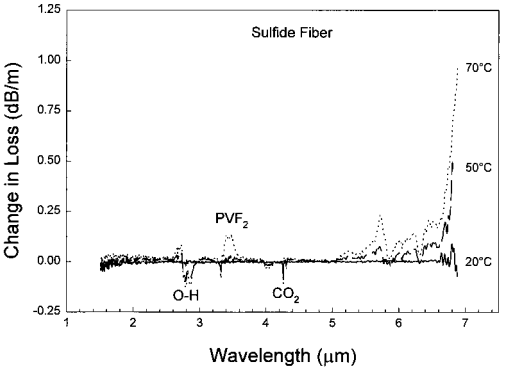

Fig. 4. Effect of heating on the change in loss of sulfide fiber. During heating for each measurement the temperature was held for 10 min to achieve equilibrium. Between 20 and 70 °C the thermally induced losses are exactly the same, i.e., reversible with temperature during heating up and during cooling down to room temperature.

Between 5 and 7 μm (Fig. 4) there are several bands separated into four groups that occur at 5.0–5.4, 5.4–5.85, 5.85–6.3, and 6.3–6.6 μm. The band group between 5.0 and 5.4 μm has been attributed to a carbene species.[10] Their origin is attributed to residual impurity carbon compounds and hydrides of S and As that remain after purification in the precursors. During high-temperature glass melting the glass precursors undergo dehydrogenation and reaction with the carbon impurity compounds according to the following transformation[10]: alkanes → alkenes (alkynes) → polyalkenes (polyalkynes) → carbene.

These reactions also enable the formation of carbon oxides, organic sulfides, and disulfide species. The bands between 5.4 and 5.85 μm are due to the vibration of the polyacetylene species.[10] The bands in the 5.85–6.3-μm region are assigned to the presence of carbon—oxygen—sulfur (COS) species (6.0 μm) and hydrides of S and As.[10] The bands in the 6.3–6.6-μm region are assigned to the vibration of molecular H_2O (6.32-μm), carbon oxides, and carbon disulfides CS_2 (6.61-μm) species.[10] The loss in these four regions increases with increasing temperature. The electromagnetic energy excites and increases the vibration of these species, which readily couple to the anharmonic interaction in the lattice, resulting in higher IR absorption. Beyond 6.6 μm the change in loss is mainly due to multiphonon absorption. The increased loss is directly due to nonlinearities in the electric dipole moment[11] and indirectly from an anharmonic interaction between IR-active phonons and photons.[12] Anharmonic interaction occurs since the number of phonons increase with temperature in accordance with the Planck distribution function $\langle n \rangle = [\exp(\hbar\omega/kT) - 1]^{-1}$. The loss increases with higher temperature in accordance with

$$\Delta\alpha_{mp} = A(T)\exp[b(T)\lambda] - A\exp(b\lambda), \qquad (3)$$

where $A(T)\exp[b(T)\lambda]$ is the multiphonon absorption at temperature T and $A\exp(b\lambda)$ is the multiphonon absorption at room temperature. $A(T)$ and $b(T)$ are material- and temperature-dependent constants and λ is the wavelength.

Figure 5 shows a comparison of the relative change in loss of the sulfide fibers at 50 °C made with high- and low-purity chemicals. For the low-purity sulfide fiber there are additional peaks at 2.9, 4.03, 4.89, and 5.0 μm that are assigned to the vibrations of O—H, H—S, C—O, and C—O—S species, respectively. Typically, for the sulfide fibers made with low-purity chemicals, the losses due to these O—H, H—S, C—O, and C—O—S impurities were approximately <3, 25, 5, and <1 dB/m, respectively. Furthermore the residual O—H in the glass gives a discernible band at ~2.9 μm in the low-purity sulfide fiber spectrum.

Figure 6 shows a change in loss in the sulfide fiber as the temperature decreases. The bands at 2.92 and 4.03 μm are due to the stretching vibration of O—H and H—S, respectively. As the temperature

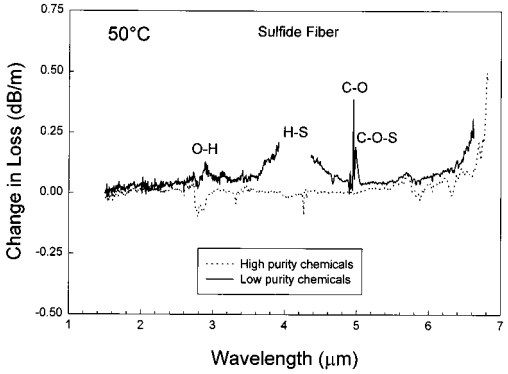

Fig. 5. Comparison between change in loss of sulfide fibers made with high- and low-purity chemicals at a temperature of 50 °C.

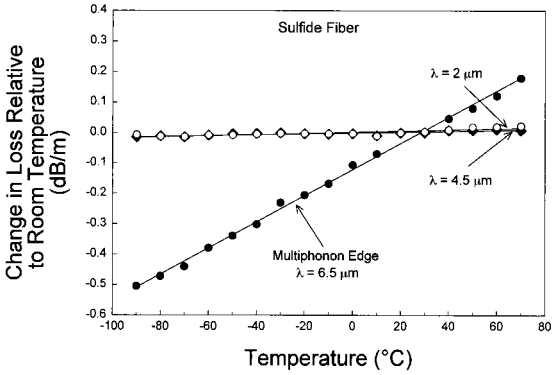

Fig. 7. Change in loss of sulfide fiber as a function of temperature at distinct wavelengths.

decreases from 20 to −90 °C the loss at these two wavelengths increases. The loss behavior at these two wavelengths is not well understood. We speculate that the loss behavior may be due to condensation of physiadsorbed H_2O on the surface of the fiber and possible hydrolysis to form an O—H and a H—S species, or it could be due to impurity-related electrically active states within the optical gap. As the temperature decreases from 20 to −90 °C the extension of the tail in the optical gap decreases. With decreasing temperature the relative energy levels of these impurity-related electrically active states overlap less within the tail, thereby making it easier for optical excitation from these impurity-related electrically active states to occur. This optical excitation causes an increased change in loss at 2.92 and 4.03 μm. Beyond 5 μm the loss of the three bands at ~5.1–5.4, 5.4–5.85, and 5.85–6.35 μm decreases. This loss is mainly due to a decrease in the coupling of IR light with IR excitation of vibrational modes of carbene (5.1–5.4 μm), polyacetylene (5.4–5.85 μm), and the COS species and the hydrides of S and As (5.85–6.35 μm), respectively. Also the multiphonon edge absorption decreases owing to fewer phonons.

Figure 7 shows a change in loss relative to room temperature of the sulfide fiber at three distinct wavelengths, namely, at 2, 4.5, and 6.5 μm. At 2 and 4.5 μm, between −90 and 60 °C the change in loss relative to room temperature is small because the sulfide fiber has a large optical gap (2.24 eV) and the free-carrier absorption and multiphonon absorption are negligible. At 6.5 μm the change in loss relative to room temperature increases and is due to multiphonon absorption. This change occurs when a photon excites the fundamental phonon–photon modes, which subsequently decays anharmonically into other secondary phonons. From Fig. 7 the temperature dependence of the change in loss, $d(\Delta\alpha)/dT$, of the sulfide fibers at $\lambda = 2$, 4.5, and 6.5 μm was calculated by linear regression to be 1.9×10^{-4}, 1.4×10^{-4}, and 4.3×10^{-3} dB/m/°C, respectively (see Table 2). For example, for an application that nominally operates at 25 °C and requires a 5-m length of sulfide fiber, the calculated changes in loss, $d(\Delta\alpha)/dT$, at $\lambda = 2$, 4.5, and 6.5 μm are 0.024, 0.018, and 0.538 dB, respectively. Therefore sulfide fibers are good candidate materials for laser power delivery in the IR (e.g., CO lasers that operate at 5.4 μm).

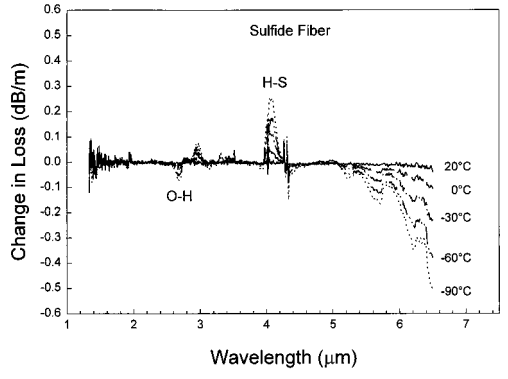

Fig. 6. Effect of cooling on the change in loss of sulfide fiber. For each measurement the temperature was held for ~5 min to achieve equilibrium. Between $20 \leq T \leq -90$ °C the thermally induced losses are exactly the same because the experiment was repeated three times with the same fiber.

Figure 8 shows the change in loss of the telluride fiber as the temperature is increased from 20 to 60 °C. The two bands at ~4.2 and 5.0 μm are due to the stretching vibration of Se—H and Ge—H,[13] respectively. In the short-wavelength cutoff region between 4 and 5 μm the loss curve follows the standard Urbach edge[14] behavior that occurs when free electrons in the mobility edge absorb sufficient photon energy and jump across the optical gap into the conduction band. The increased loss increases with

Table 2. Temperature Dependence of the Change in Loss of Telluride and Sulfide Glasses

Fiber Type	λ (μm)	$d(\Delta\alpha)/dT$ (dB/m/°C)
Sulfide	2.0	1.9×10^{-4}
	4.5	1.4×10^{-4}
	6.5	4.3×10^{-3}
Telluride	4.1	4.4×10^{-2}
	8.0	2.0×10^{-3}
	10.6	1.9×10^{-2}

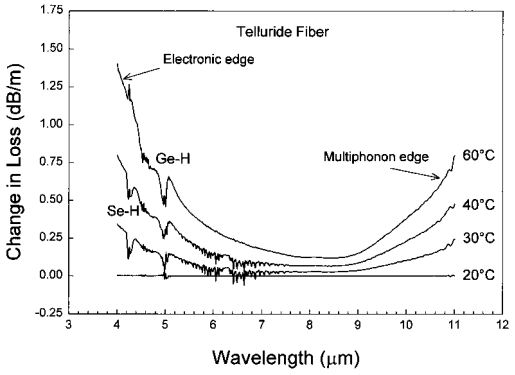

Fig. 8. Effect of heating on the change in loss of telluride fiber. During heating for each measurement the temperature was held for 10 min to achieve equilibrium. Between 20 and 60 °C the thermally induced losses are exactly the same during heating up and during cooling down to room temperature.

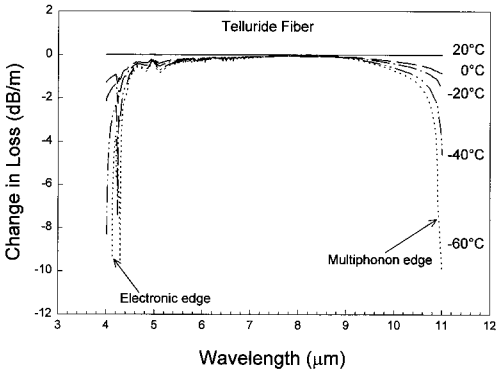

Fig. 9. Effect of cooling on the change in loss of telluride fiber. For each measurement the temperature was held at ~5 min to achieve equilibrium. Between $20 \leq T \leq -60$ °C the thermally induced losses are exactly the same because the experiment was repeated three times with the same fiber.

higher temperature in accordance with the following empirical relationship:

$$\Delta\alpha_{\mathrm{el}} = C(T)\exp[d(T)/\lambda] - C\exp(\mathrm{d}/\lambda), \qquad (4)$$

where $C(T)\exp[\mathrm{d}(T)/\lambda]$ is the electronic absorption at temperature T and $C\exp(\mathrm{d}/\lambda)$ is the electronic absorption at room temperature. $C(T)$ and $\mathrm{d}(T)$ are material- and temperature-dependent constants.

In the tellurium-based glass, since tellurium possesses a semimetallic character, the free-electron concentration increases with temperature because of the smaller optical gap ($E_0 = 1.17$ eV). Depending on the temperature, this free-electron concentration would contribute to the overall loss spectrum as free-carrier absorption. The free-carrier absorption is an indirect process that involves both a photon and a phonon. This indirect process occurs when electrons in the lower conduction band absorb the incident electromagnetic radiation and are excited to the higher-lying conduction bands (intraband absorption) or states in different bands (interband absorption). As the temperature increases, these electrons are scattered inelastically by lattice vibrations, transferring energy to the lattice of the material. The intraband absorption α_{fc} follows the empirical relationship[15]:

$$\alpha_{fc} = G\lambda^{m}, \qquad (5)$$

where G is the constant for optical phonon scattering and m lies between $1.5 \leq m \leq 3.5$. Materials with a higher carrier mobility have a larger m value. The absorption depends on the free-carrier concentration that obeys Fermi statistics. From Fig. 8 at $T \geq 30$ °C in the electronic edge region ($\lambda = 4.1$ μm) the change in loss is due to both electronic and free-carrier absorption, i.e., $\Delta\alpha(T) = \Delta\alpha_{\mathrm{el}}(T) + \Delta\alpha_{\mathrm{fc}}(T)$. At $T = 30$ °C the change in loss is predominantly due to electronic absorption, whereas at $T = 60$ °C both the electronic and the free-carrier absorption contributed to the total loss. Between the electronic and the multiphonon edges ($\lambda = 6$–9 μm) the change in loss is mainly due to free-carrier absorption. In addition Rayleigh scattering also contributes to the total loss, but the contribution is very small and is discussed below. At $T = 60$ °C and beyond 9 μm the change in loss associated with the long-wavelength absorption edge is due to free-carrier absorption and multiphonon absorption, i.e., $\Delta\alpha(T) = \Delta\alpha_{\mathrm{mp}}(T) + \Delta\alpha_{\mathrm{fc}}(T)$. The mechanism of multiphonon absorption for the telluride fiber is the same as that of the sulfide fiber discussed above. Inagawa *et al.*[16] have shown that for the Ge–As–Se–Te glass system the activation energies for the multiphonon and free-carrier absorption are 0.06 eV (23–67 °C) and 0.01 eV (77–127 °C), respectively. Figure 8 shows that for the telluride fiber at $T \leq 60$ °C the increase in loss beyond 9 μm is mainly due to multiphonon absorption. At $T = 60$ °C there is a small contribution of free-carrier intraband absorption to the overall change in loss. Although no measurement was taken for $T > 60$ °C it is expected that at $T \geq 80$ °C free-carrier absorption is more dominant than multiphonon absorption based on its smaller activation energy.[16]

Figure 9 shows the change in loss of the telluride fiber as the temperature decreases from 20 to −60 °C. For the Urbach edge region ($\lambda \leq 4.2$ μm) the loss decreases and is due to less thermally activated free electrons in the mobility edge able to jump across the gap into the conduction band. Also, since the tellurium-based glass possesses a semimetallic character, the optical gap widens as the temperature decreases and the excitation of free electrons in the mobility edge and excitation of bound valence electrons into the conduction band becomes less likely. Between the short- and the long-wavelength region (6–9 μm) the overall change in loss is negligible; i.e., the effect of free-carrier absorption is small since free carriers are thermally activated. Beyond 10 μm the telluride fiber becomes more transparent with cooling owing to reduced multiphonon absorption. This increased transparency is due to less anharmonic interaction since the number of phonons $\langle n \rangle$ available is lower.

Figure 10 shows the change in loss relative to room

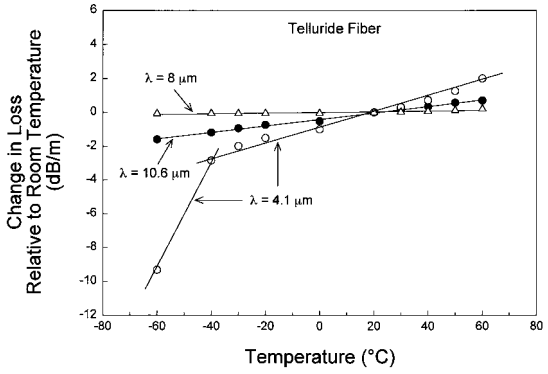

Fig. 10. Change in loss of telluride fiber as a function of temperature at distinct wavelengths.

temperature of the telluride fiber at three distinct wavelengths of 4.1, 8.0, and 11 μm. At the electronic-edge region (λ = 4.1 μm), for −40 °C ≤ T ≤ 60 °C, a larger slope in the change in loss relative to room temperature was observed (compared with λ = 8, 10.6 μm). This larger slope occurs because the telluride fiber has a small optical gap (E_0 = 1.17 eV at 22 °C), and so electronic and free-carrier absorption can occur easily. Below $T \leq -40$ °C there appears to be a sharp decrease in loss. This decrease could possibly be due to the widening of the optical gap as the temperature decreases or the contribution of free-carrier absorption being very small. In the minimum loss region (λ = 8.0 μm) there is a small increase in the change in loss relative to room temperature. For comparison the minimum loss region of the telluride fiber (λ = 8.0 μm) has a larger increase in loss than the sulfide fiber (λ = 4.5 μm) for $T \geq 30$ °C. This increase is due to a higher free-carrier absorption associated with a higher free-electron concentration in the telluride fiber. At the multiphonon-edge region (λ = 10.6 μm), as the temperature increases from −60 to 40 °C, thermal vibration and anharmonic interaction between IR-active phonons and photons increase coupling with IR absorption, resulting in a sharp increase in loss relative to room temperature. At $T \geq 60$ °C a small contribution of free-carrier absorption together with a large contribution of multiphonon absorption accounts for the total absorption loss in the telluride fiber. From Fig. 10, when linear regression is used, the temperature dependence of the change in loss, $d(\Delta\alpha)/dT$, of the telluride fibers at λ = 4.1, 8, and 10.6 μm was calculated to be 4.4×10^{-2}, 2.0×10^{-3}, and 1.9×10^{-2} dB/m/°C, respectively (see Table 2). Again, if we consider an application that nominally operates at 25 °C and that requires 5 m of telluride fiber, the calculated changes in loss, $d(\Delta\alpha)/dT$, at λ = 4.1, 8, and 10.6 μm are 5.50, 0.25, and 2.38 dB, respectively. The relatively large change in loss limits the lengths that could be used in the laser power delivery of CO_2 lasers that operate at 10.6 μm. Chemical-sensing applications in the 6–9-μm region can still be performed with a minimal change in loss.

Impurities also contribute to the total loss of the fiber since impurities introduce states in the optical gap. As the temperature increases, the presence of these states in the gap makes it easier for impurity-related absorption to occur. However, the exact nature of this impurity-related absorption is complicated and is not treated in this study, although their potential effects are shown in Fig. 5. On the other hand, the extent of Rayleigh scattering is known and can be estimated for the sulfide and the telluride fibers. Rayleigh scattering occurs as a result of compositional and density fluctuations in the material on a microscopic level, which leads to localized changes in the dielectric constant. This fluctuation in the dielectric constant and variation in the refractive index lead to Rayleigh scattering that has a λ^{-4} wavelength dependence. The Rayleigh-scattering contribution is derived theoretically[17] as

$$\alpha_{\mathrm{RS}} = \frac{8}{3}\frac{\pi^3}{\lambda^4} n^8 p^2 \beta_T k_B T_g = \frac{C_{\mathrm{RS}}}{\lambda^4}, \tag{6}$$

where n is the index of refraction, p is the photoelastic Pockels constant, β_T is the isothermal compressibility, k_B is the Boltzmann constant, T_g is the glass-transition temperature, and C_{RS} is the Rayleigh-scattering coefficient. By taking the first derivative of Eq. (6), the loss with respect to temperature due to Rayleigh scattering, $d(\alpha_{\mathrm{RS}})/dT$, is calculated to be $Wn^7 T_g (dn/dT)/\lambda^4$, where $W = (64\pi^3 p^2 \beta_T k_B)/3$, and assumes that p and β_T are constant. For the sulfide and the telluride fibers, $d(\alpha_{RS})/dT$ is determined and listed in Table 3 with the value of $p = 0.3$,[18] $\beta_T = 10^{11}$ dyn/cm^2,[19] $k_B = 1.38 \times 10^{-23}$ J/K, $n = 2.41$ (sulfide), 2.95 (telluride),[16] T_g = 473 K (sulfide), 538 K (telluride), and $dn/dT = 1 \times 10^{-5}$ K^{-1} (sulfide), 9×10^{-5} K^{-1} (telluride).[16] At T = 70 °C for a 5-m-long sulfide fiber between 1 and 5 μm the change in loss due to Rayleigh scattering, $d\alpha_{RS}$, is calculated to be less than 3.0×10^{-8} dB. Similarly at T = 60 °C for a 5-m-long telluride fiber, between 5 and 9 μm, $d\alpha_{RS}$ is calculated to be less than 2×10^{-9} dB. Thus one can see that the loss due to changes in Rayleigh scattering is very small in the sulfide and the telluride fibers and therefore can be neglected.

Table 3. Loss with Respect to Temperature Owing to Rayleigh Scattering, $d(\alpha_{RS})/dT$

Fiber Type	$d(\alpha_{\mathrm{RS}})/dT$ (dB/m/K)
Sulfide	$1.8 \times 10^{-11}/\lambda^4$
Telluride	$7.6 \times 10^{-10}/\lambda^4$

5. Conclusions

The change in loss of the sulfide glass fibers is smaller than that of the telluride glass fibers as a function of temperature, because the sulfide glass has a much larger optical gap and less free-carrier absorption. Also since tellurium exhibits a semimetallic character, telluride glass fiber has a greater free-electron concentration than that of the sulfide glass fiber. The smaller optical gap and the larger free-electron

concentration possessed by the telluride glass fiber makes it possible for thermally activated free electrons to be excited from the valence to the conduction band and increases the loss in the region of the electronic absorption edge ($\lambda \leq 4.1$ μm). In addition to this, between wavelengths of 6 and 9 μm the telluride fibers exhibit a noticeable free-carrier absorption above 30 °C, unlike the sulfide fiber. The long-wavelength edge ($\lambda \geq 9$ μm) is dominated by multiphonon absorption at $T \leq 60$ °C. At $T \geq 80$ °C it is expected that free-carrier absorption is dominant based on the activation energy data. Therefore, owing to a higher temperature dependence on the change in loss, telluride fibers are good for chemical sensings at temperatures of less than 30 °C. Since sulfide fibers possess low-temperature dependence on the change in loss, they are currently being used in IR countermeasures and laser threat-warning systems.

The authors acknowledge the work of P. Pureza in drawing the fibers and R. Miklos in fabricating the telluride and the sulfide tubes. Also, we thank David Schaafsma and Brandon Shaw for comments and discussion.

References

1. J. R. Gannon, "Materials for mid-infrared waveguides," in *Infrared Fibers*, L. G. DeShazer, ed., Proc. SPIE **266,** 62–68 (1981).
2. J. S. Sanghera, F. H. Kung, L. E. Busse, P. C. Pureza, and I. D. Aggarwal, "Infrared evanescent absorption spectroscopy of toxic chemicals using chalcogenide glass fibers," J. Am. Ceram. Soc. **78,** 2198–2202 (1995).
3. G. Nau, F. Bucholtz, K. J. Ewing, S. T. Vohra, J. S. Sanghera, and I. D. Aggarwal, "Fiber optic IR reflectance sensor for the cone penetrometer," in *Environmental Monitoring and Hazardous Waste Site Remediation*, T. V. Dinh, ed., Proc. SPIE **2504,** 291–296 (1995).
4. L. E. Busse, J. S. Sanghera, and I. D. Aggarwal, "High optical power transmission through glass cladded infrared fiber," in *Proceedings of the 1994 Infrared Information Symposia Specialty Group Infrared Materials* (Environmental Research Institute of Michigan, Ann Arbor, Mich., 1995), p. 341.
5. J. S. Sanghera, I. D. Aggarwal, L. E. Busse, P. C. Pureza, V. Q. Nguyen, R. Miklos, F. H. Kung, and R. Mossadegh, "Development of low loss IR transmitting chalcogenide glass fibers," in *Biomedical Optoelectronic Instrumentation*, A. Katzir, A. Harrington, and D. M. Harris, eds., Proc. SPIE **2396,** 71–77 (1995).
6. L. E. Busse, J. Moon, J. S. Sanghera, and I. D. Aggarwal, "Chalcogenide fibers deliver high IR power," Laser World Focus **32,** 143–150 (1996).
7. J. S. Sanghera, V. Q. Nguyen, P. C. Pureza, F. H. Kung, R. Miklos, and I. D. Aggarwal, "Fabrication of low-loss IR-transmitting $Ge_{30}As_{10}Se_{30}Te_{30}$ glass fibers," J. Lightwave Technol. **12,** 737–741 (1994).
8. J. S. Sanghera, V. Q. Nguyen, P. C. Pureza, R. Miklos, F. H. Kung, and I. D. Aggarwal, "Fabrication of long lengths of low-loss IR transmitting $As_{40}S_{(60-x)}Se_x$ glass fibers," J. Lightwave Technol. **14,** 743–748 (1996).
9. J. Tauc, R. Grigorovici, and A. Vancu, "Optical properties of electronic structure of amorphous germanium," Phys. Status Solidi **15,** 627–637 (1966).
10. M. F. Churbanov, "High purity chalcogenide glasses as material for fiber optics," J. Non-Cryst. Solids **184,** 25–29 (1995).
11. M. Lax and E. Burstein, "Infrared lattice absorption in ionic and homopolar crystals," Phys. Rev. **97,** 39–52 (1955).
12. M. Born and K. Huang, *Dynamical Theory of Crystal Lattices* (Oxford University, London, 1954).
13. G. G. Devyatykh, M. F. Churbanov, I. V. Scripachev, E. M. Dianov, and V. G. Plotnichenko, "Middle infrared As–S, As–Se, Ge–As–Se chalcogenide glass fibers," Int. J. Optoelectron. **7,** 237–254 (1992).
14. F. Urbach, "The long-wavelength edge of photographic sensitivity and of the electronic absorption of solids," Phys. Rev. **92,** 1324–1325 (1953).
15. J. I. Pankove, *Optical Processes in Semiconductors* (Dover, New York, 1971).
16. I. Inagawa, S. Moromoto, T. Yamashita, and I. Shirotani, "Temperature dependence of transmission loss of chalcogenide glass fibers," Jpn. J. Appl. Phys. **36,** 2229–2235 (1997).
17. R. Olshansky, "Propagation in glass optical waveguides," Rev. Mod. Phys. **51,** 341–367 (1979).
18. M. E. Lines, "Physical properties of materials: theoretical overview," in *Handbook of Infrared Optical Materials*, P. Klocek, ed. (Marcel Dekker, New York, 1991).
19. N. W. Ashcroft and N. D. Mermin, *Solid State Physics* (Holt, Rinehart, Winston, New York, 1976).